Entangled-Beam reflectometry and Goos-Hänchen Shift

G. Ortiz,[1] Q. Le Thien,[1] and R. Pynn[1]
[1] *Department of Physics, Indiana University, Bloomington, IN 47405, USA**

v2

CONTENTS

I. Introduction: the entangled neutron beam as a probe of correlated matter 1

References 5

Supplemental Material: Entangled-Beam reflectometry and Goos-Hänchen Shift 5

A. Neutron optics with spin 5
1. Wave Packet 6
2. 2nd-order correction to the GH-shift 7

B. Probing Surface Magnetic Field 8

I. INTRODUCTION: THE ENTANGLED NEUTRON BEAM AS A PROBE OF CORRELATED MATTER

Within Pleshanov
Step 1: Standard GH shift with one interface
Step 2: GH shift with several interfaces
Step 3: EGH shift with one interface
Step 4: EGH shift with several interfaces
Imbert-Fedorov shift
Goals/targets

- the transverse coherence length of the neutron
- from entangled reflectometry, can we infer magnetic properties of the surface
- negative "magnetic" index of refraction ?

In the following we are assuming that one is working in the optical potential approximation, where the medium represents a constant refractive index.

For a general derivation see Appendix XXX. We start illustrating the technique in the case of a single magnetic layer.

With the recent advances of spin echo technique using either Magnetic-Wollaston Prisms (MWP) [] or RF-flippers [] to entangle a neutron in path and spin.

Introduction.— The Goos-Hänchen shift (GH-shift) refers to the in-plane lateral shift, λ_x, of the center of a beam of waves undergoing total internal reflection (TIR) from a surface (see Fig. 1). This phenomenon was first predicted for light by Sir Isaac Newton [1] and measured by Goos and Hänchen in 1947 [2, 3]. Recently, de Haan *et al.* [6] claimed observation of that effect in neutron optics. The first theoretical description of the phenomenon focused on the phase shift $\Phi(\mathbf{k}_0)$ of an incoming plane wave of momentum $\mathbf{k}_0 = (k_{0x}, k_{0y}, k_{0z})$ undergoing TIR, within the stationary phase method [4],

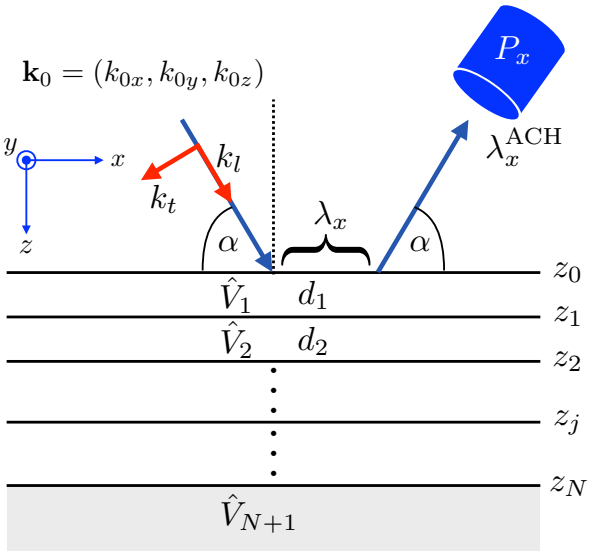

FIG. 1. Schematics of a typical setup for measuring the GH-shift. An incoming wave of mean momentum $\mathbf{k}_0$ impinges on a surface and gets reflected carrying information about the surface. Geometric, λ_x, and phase, $\lambda_x^{\rm ACH}$, GH shifts are indicated. Allowed magnetic structures along the z-axis are simply characterized by a stratified medium with homogeneous layers (of width d_j and optical potential V_j) labeled by the index $j = 1, 2, \cdots, N$. Momenta along the x-z and l-t frames are related by $k_x = k_l \cos\alpha$, $k_z = k_l \sin\alpha$.

$$\lambda_x^{\rm ACH} \equiv \frac{k_{0x}}{k_{0z}} \frac{d\Phi(\mathbf{k}_0)}{dk_{0z}}, \tag{1}$$

expression known as the Artmann-Carter-Hora (ACH) formula [4, 5]. The connection between this and the geometric spatial shift λ_x [13] was made by arguing that $\lambda_x^{\rm ACH}$ could be expressed as the effective displacement (along the x-axis in Fig. 1) resulting from the group delay time τ the wave experiences between arrival and departure from the surface, first noted by Agudín [14],

$$\lambda_x^{\rm ACH} = \frac{k_{0x}}{m} \frac{d\Phi(\mathbf{k}_0)}{dE_z} = v_x \tau \equiv \lambda_x, \tag{2}$$

* ortizg@iu.edu

where $2mE_z = k_{0z}^2$ and $mv_x = k_{0x}$, assuming non-relativistic particles of mass m ($\hbar = 1$). It is important to emphasize, however, that a geometric GH-shift has a physical meaning only if the beam has a finite width, making the identification above questionable. Since these original contributions various attempts at deriving such a geometric shift using wave packets have been advanced in the literature [7–9, 12].

Measuring the Goos-Hänchen Shift.— A natural question that emerges is why does the GH-shift seems to be independent of the wave packet width? We next illustrate by means of an elliptical wave packet analysis that this is not the case in general. Our motivation to consider such a wave packet is grounded on available experimental evidence, for example, in neutron beams where longitudinal, Δ_l, and transverse, Δ_t coherence lengths differ substantially [17].

Consider an incoming wave packet, centered at $\mathbf{r}_c = (x_c, z_c)$, in momentum space ($\mathcal{N}$ is a normalization factor)

$$\Psi^{(\mathrm{i})}(\mathbf{k}) = \mathcal{N}\, e^{-\frac{\Delta_x^2}{2}(k_x-k_{0x})^2-\frac{\Delta_z^2}{2}(k_z-\bar{k}_{0z})^2-i\mathbf{k}\cdot\mathbf{r}_c}, \quad (3)$$

where, for the sake of clarity, we only write down coordinates in the scattering xz-plane (Fig. 1) and omit spinor notation for now. Here,

$$\Delta_z = \sqrt{\Delta_l^2 \sin^2\alpha + \Delta_t^2 \cos^2\alpha}, \quad \Delta_x\Delta_z = \Delta_l\Delta_t, \quad (4)$$

and the Gaussian along k_z peaks at

$$\bar{k}_{0z} = \frac{\sin\alpha\left(\Delta_l^2 k_{0l} - k_x\cos\alpha\left(\Delta_l^2-\Delta_t^2\right)\right)}{\Delta_z^2}. \quad (5)$$

This wave packet gets reflected by a surface whose reflection coefficient $R(k_z)$ only depends on the momentum component normal to the surface because of translation symmetry along the x direction. The resulting reflected wave packet

$$\Psi^{(\mathrm{r})}(\mathbf{k}) = \Psi^{(\mathrm{i})}(\mathbf{k})R(k_z) = \Psi^{(\mathrm{i})}(\mathbf{k})\; e^{i\Phi}, \quad (6)$$

can be expressed in terms of a momentum-dependent phase shift $\Phi(\mathbf{k}) \in \mathbb{R}$. Assuming the width of the incident wave packet normal to the surface to be larger than the semi-classical penetration depth

$$\lambda_z(k_z) = -\frac{i}{2}\frac{d\ln R}{dk_z} \ll \Delta_z, \quad (7)$$

one can expand Φ (up to second order) about $\bar{k}_{0z}$

$$\Phi(\mathbf{k}) = -i\ln\bar{R} + 2\bar{\lambda}_z(k_z-\bar{k}_{0z}) + \overline{W}^2(k_z-\bar{k}_{0z})^2, \quad (8)$$

where

$$W^2(k_z) = -\frac{i}{2}\frac{d^2\ln R}{dk_z^2}, \quad (9)$$

and $\bar{R}$, $\bar{\lambda}_z$, $\overline{W}^2$ are evaluated at $k_z = \bar{k}_{0z}$.

The reflected time, t, dependent wave function in coordinate representation,

$$\Psi^{(\mathrm{r})}(\mathbf{r},t) = \int d\mathbf{k}\; \Psi^{(\mathrm{r})}(\mathbf{k})\; e^{i(\mathbf{k}^{(\mathrm{r})}\cdot\mathbf{r}-\frac{k^{(\mathrm{r})2}}{2m}t)}, \quad (10)$$

carries information about the interaction with the surface, where we define $\mathbf{k}^{(\mathrm{r})} = (k_x, -k_z)$ for convenience due to reflection, this superscript prescription also extends to other specific momenta. Notice that, in the elliptical wave packet case, $\Psi^{(\mathrm{r})}(\mathbf{r},t)$ intertwines the x and z coordinates due to the k_x dependence in $\bar{k}_{0z}$. While the incoming wave packet is separable in longitudinal and transverse components, this is no longer the case for the reflected wave function. This can be shown analytically if one ignores the second-order correction $\overline{W}^2$, since $\Psi^{(\mathrm{r})}(\mathbf{r},t)$ can then be resolved in closed form.

To further proceed, we next consider the quasi-spherical approximation

$$\frac{\Delta_l^2-\Delta_t^2}{\Delta_l^2} \ll \frac{k_{0l}}{k_{0x}\cos\alpha} = \frac{1}{\cos^2\alpha}, \quad (11)$$

where we made use of the dominant x-momentum k_{0x} (see Eq. (3)). Then, $\bar{k}_{0z}$ becomes

$$\bar{k}_{0z} \approx \tilde{k}_{0z} = \left(\frac{\Delta_l}{\Delta_z}\right)^2 k_{0l}\sin\alpha = \left(\frac{\Delta_l}{\Delta_z}\right)^2 k_{0z}, \quad (12)$$

where to lowest-order, the ellipticity in the incoming wave packet simply renormalizes the dominant normal momentum to $\tilde{k}_{0z}$. This replacement, $\bar{k}_{0z} \to \tilde{k}_{0z}$, extends to all other quantities which are dependent on $\bar{k}_{0z}$, such as $\widetilde{\Phi}$, $\tilde{\lambda}$ and $\widetilde{W}$. Using this quasi-spherical approximation, the integral in Eq. (10) becomes now separable in x and z

$$\Psi^{(\mathrm{r})}(\mathbf{r},t) \approx \tilde{R}\, e^{-2i\tilde{k}_{0z}\tilde{\lambda}_z}\Psi_x(x,t)\Psi_z(z,t), \quad (13)$$

where $\Psi_x(x,t)$ is the usual Gaussian wave packet of initial width Δ_x, and mean momentum k_{0x}, and $\Psi_z(z,t)$ the modified Gaussian wave packet

$$\Psi_z(z,t) = \mathcal{N}(t)\, e^{-\frac{(z+z_c-2\tilde{\lambda}_z+\tilde{k}_{0z}t/m)^2}{2\Delta_z^2(t)}+i\,\tilde{\phi}(z,t)}, \quad (14)$$

with modified t-dependent normalization $\mathcal{N}(t)$, dispersion $\Delta_z(t)$ and phase $\tilde{\phi}(z,t)$ having a complicated dependence on t and Δ_z. The reflected wave packet centers about $\mathbf{r}^{(\mathrm{r})}(t) = (0, 2\tilde{\lambda}_z) + \mathbf{r}_c^{(\mathrm{r})} + \frac{\tilde{\mathbf{k}}_0^{(\mathrm{r})}}{m}t$, where $\mathbf{r}_c^{(\mathrm{r})} = (x_c, -z_c)$. Note that $\tilde{\mathbf{k}}_0^{(\mathrm{r})} = (k_{0x}, -\tilde{k}_{0z})$.

We are now in a position to respond to our original question. From Eq. (13) the geometric GH-shift, defined as the displacement of the wave packet center along the x axis during the group delay time τ, is given by

$$\lambda_x = \frac{k_{0x}}{m}\frac{2\tilde{\lambda}_z}{\tilde{k}_{0z}/m} = \left(\frac{\Delta_z}{\Delta_l}\right)^2 2\tilde{\lambda}_z\cot\alpha, \quad (15)$$

which clearly displays a wave packet width dependence. Interestingly, the width dependence disappears for a spherical wave packet.

We now turn to consider the effect of the second-order term $\widetilde{W}^2$, on the GH-shift, within the quasi-spherical approximation. Firstly, the dispersion along the z-direction becomes

$$\Delta_z(t) = \Delta_z\sqrt{1+\frac{1}{m^2\Delta_z^4}\left[t-2m\widetilde{W}^2\right]^2}, \qquad (16)$$

which shows that the second-order term reduces the effective expansion time of the wave packet. For neutron beams reflected off a semi-infinite slab with a constant potential its contribution is given by $\widetilde{W}^2 = \tilde{k}_{0z}\tilde{\lambda}_z^3$, indicating its relevance for precision-measurement experiments involving mirrors (as in Mach-Zehnder interferometers) that have large penetration depths. If the slab is magnetic, as we will see, its effect will be different on the two spin components of the neutron wave packet, thus affecting the measurement visibility at the detector.

Secondly, while the exact phase-shift has a complicated dependence on the evolution time t and the initial wave packet widths Δ_x and Δ_z, due to wave packet dispersion, a far-field observer ($t/m \gg \Delta_z^2, \widetilde{W}^2$) will measure the asymptotic reflection phase-shift

$$S \equiv \lim_{t\to\infty} \mathrm{Arg}\left[\Psi^{(\mathrm{r})}(\mathbf{r},t)\right] = \widetilde{\Phi} + 4\tilde{k}_{0z}^2\widetilde{W}^2 \qquad (17)$$

where we have ignored the plane wave phase. Due to this additional correction the measured λ_x^{ACH} should differ from the geometric shift in Eq. (15). This is because $\widetilde{W}^2$ does not shift the center of the wave packet. Therefore, to make connection to the ACH formula analysis of Eq. (1) one needs to take this correction into account

$$\lambda_x^{\mathrm{ACH}} \equiv \frac{k_{0x}}{\tilde{k}_{0z}}\frac{d\widetilde{\Phi}}{d\tilde{k}_{0z}} = \frac{k_{0x}}{\tilde{k}_{0z}}\frac{d}{d\tilde{k}_{0z}}\left(S - 4\tilde{k}_{0z}^2\widetilde{W}^2\right) = \lambda_x. \qquad (18)$$

Since $\widetilde{W}^2$ grows with the penetration depth $\tilde{\lambda}_z$, one must take into account this correction to the ACH formula for reflections close to the critical angle, such as in de Haan *et al.*'s experiment [6]. Table I summarizes our findings.

[Quan: We note that the $\widetilde{W}$-correction to the observed phase-shift is unique to the wave packet treatment, i.e. no treatment of plane wave can yield this term. Hence, if one can observe the presence of this correction, one can in principle distinguish whether the incoming state is a wave packet or a plane wave. Interestingly, while having its origin from the wave packet nature, the $\widetilde{W}$-correction is independent of the incoming wave packet's width in the asymptotic limit.]

The Entangled Goos-Hänchen Effect.— We now turn to examine the GH-shift for an incoming mode-entangled, in spin (or polarization) and path, state [15]

$$\Psi_{\boldsymbol{\xi}}^{(\mathrm{i})}(\mathbf{k}) = \Psi^{(\mathrm{i})}(\mathbf{k}) \otimes \boldsymbol{\chi}_{\mathbf{k}\cdot\boldsymbol{\xi}}^{(\mathrm{i})}\,, \qquad (19)$$

where the two-component spinor $\boldsymbol{\chi}_{\mathbf{k}\cdot\boldsymbol{\xi}}^{(\mathrm{i})} = \frac{1}{\sqrt{2}}\begin{pmatrix} e^{-i\mathbf{k}\cdot\boldsymbol{\xi}^{(\mathrm{i})}/2} \\ e^{i\mathbf{k}\cdot\boldsymbol{\xi}^{(\mathrm{i})}/2}\end{pmatrix}$, written in the σ_z-basis ($|\uparrow\rangle$ and $|\downarrow\rangle$), carries information about the displacement vector $\boldsymbol{\xi}^{(\mathrm{i})}$ separating the centers of the two incoming coherent wave packets (Fig. 2). Upon TIR from a magnetic (or birefringent) material surface, the reflection operator $\hat{R}(k_z) = \mathrm{diag}(R_+, R_-)$, in its orthonormal eigenbasis $|\pm\rangle$, defines an effective quantization axis $\hat{n} = (\sin\theta\cos\phi, \sin\theta\sin\phi, \cos\theta)$, where ϕ and θ are the usual Bloch sphere angles [18]. The two bases are related by a unitary unimodular rotation $\mathbf{U}(\theta,\phi)$: $(|+\rangle \;\; |-\rangle)^{\mathrm{T}} = \mathbf{U}^{\mathrm{T}}(\theta,\phi)(|\uparrow\rangle \;\; |\downarrow\rangle)^{\mathrm{T}}$. Hence, the reflected wave function is given, in the surface $|\pm\rangle$-basis, by

$$\Psi_{\boldsymbol{\xi}}^{(\mathrm{r})}(\mathbf{r},t) = \int d\mathbf{k}\; \hat{R}(k_z)\mathbf{U}^{\dagger}\Psi_{\boldsymbol{\xi}}^{(\mathrm{i})}(\mathbf{k})\; e^{i(\mathbf{k}^{(\mathrm{r})}\cdot\mathbf{r} - \frac{k^{(\mathrm{r})2}}{2m}t)}. \qquad (20)$$

In the quasi-spherical limit the reflected state can be expressed as [Quan:

$$\Psi_{\boldsymbol{\xi}}^{(\mathrm{r})}(\mathbf{r},t) = \sum_{\mu,\nu=\pm} \mathbf{U}_{\mu\nu}^{*}\Psi_{\mu\nu}^{(\mathrm{r})}(\mathbf{r},t)\otimes|\nu\rangle\,,$$

] where $\mathbf{U} = \begin{pmatrix} \cos\frac{\theta}{2} & -e^{-i\phi}\sin\frac{\theta}{2} \\ e^{i\phi}\sin\frac{\theta}{2} & \cos\frac{\theta}{2}\end{pmatrix}$, and $\Psi_{\mu\nu}^{(\mathrm{r})}(\mathbf{r},t)$ is defined as the $\Psi^{(\mathrm{r})}(\mathbf{r},t)$ (Eq. (13)) but centered about $\mathbf{r}_{\mu\nu}(t) = \frac{\boldsymbol{\xi}_\mu}{2} + (0,2\tilde{\lambda}_\nu) + \mathbf{r}_c^{(\mathrm{r})} + \frac{\tilde{\mathbf{k}}_0^{(\mathrm{r})}}{m}t$, with $\boldsymbol{\xi}_\mu = \mu(\xi_x^{(\mathrm{i})}, -\xi_z^{(\mathrm{i})})$. Indices μ and ν carry a physical meaning; while μ represents a polarization index along the incoming spin-basis, ν is associated to the reflected one. Hence, upon TIR, an incoming μ spin state is split into $\Psi_{\mu+}^{(\mathrm{r})}$ and $\Psi_{\mu-}^{(\mathrm{r})}$, with centers separated by $2(\tilde{\lambda}_+ - \tilde{\lambda}_-)\hat{z}$ due to experiencing different GH-shifts.

Two physical effects can be identified in Eq. (21). The first concerns the generated entanglement pattern. Generically, the reflected state splits coherently into four wave packets, yet it remains mode-entangled with respect to the distinguishable path and spin subsystems decomposition. In conjunction with MWPs and radio-frequency flippers, this effect can be exploited to generate arbitrary mode-entangled beams. Secondly, if the incoming wave packet is entangled in the same spin-basis as the reflected eigenstates ($\phi, \theta = 0$), there will only be two reflected wave packets $\Psi_{++}^{(\mathrm{r})}$ and $\Psi_{--}^{(\mathrm{r})}$, separated by a reflected entanglement vector $\boldsymbol{\xi}^{(\mathrm{r})} = \mathbf{r}_{++}(t) - \mathbf{r}_{--}(t)$,

$$\xi_z^{(\mathrm{r})} = -\xi_z^{(\mathrm{i})} + 2(\tilde{\lambda}_+ - \tilde{\lambda}_-), \quad \xi_x^{(\mathrm{r})} = \xi_x^{(\mathrm{i})}, \qquad (21)$$

	$\lambda_x^{\mathrm{ACH}}\ (t\to\infty)$	λ_x
PW	$2\lambda_z(k_{0z})\cot\alpha$	N/A
SWP	$2\lambda_z(k_{0z})\cot\alpha$	$2\lambda_z(k_{0z})\cot\alpha$
EWP	$\left(\frac{\Delta_z}{\Delta_l}\right)^2 2\tilde{\lambda}_z\cot\alpha$	$\left(\frac{\Delta_z}{\Delta_l}\right)^2 2\tilde{\lambda}_z\cot\alpha$

TABLE I. GH-shift for different incoming states (PW: plane wave, SWP: Spherical wave packet and EWP: Elliptical wave packet). The ACH formula, λ_x^{ACH}, is derived from the asymptotic reflection phase-shift $\overline{\Phi}(\tilde{\mathbf{k}}_0)$ measured at $t\to\infty$.

Hence, the distance between the two wave packet centers, i.e., the entanglement length [15], can be increased or decreased depending on the difference between the spin-dependent penetration depths. [Quan: Furthermore, in this particular case one can identify a simple physical picture to the entangled GH-shift, i.e. each eigen spin state along the surface quantization axis $\hat{n}$ experiences the corresponding GH-shift $\lambda_{x\pm}$ as shown in Fig. 2.]

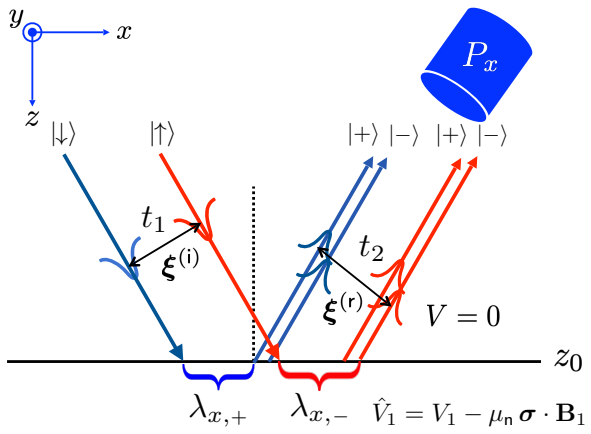

FIG. 2. Schematics of a proposed setup for measuring the Entangled GH-shift.

We next describe a way to extract the GH-shift from polarization measurements performed at the far-field as in Fig. 2. The measured x-polarization, where we picked a particular axis without a loss in generality, can be expressed as the sum

$$\lim_{t\to\infty}\vec{P}(t) = \tfrac{1}{2}\sum_{\mu,\mu',\nu,\nu'=\pm}\mathbf{U}_{\mu\nu}\mathbf{U}^*_{\mu'\nu'}\langle\nu|\,\vec{\sigma}\,|\nu'\rangle\, P^{\mu\mu'\nu\nu'} \tag{22}$$

where $P_x^{\mu\mu'\nu\nu'}$ is given by

$$P^{\mu\mu'\nu\nu'}(t) = \int d\mathbf{r}\ \Psi^{(\mathrm{r})*}_{\mu\nu}(\mathbf{r},t)\Psi^{(\mathrm{r})}_{\mu'\nu'}(\mathbf{r},t) \tag{23}$$

In the far-field limit within the quasi-spherical approximation, there is a significant simplification, because the non-trivial reflection phase shift $S_{\mu\nu}$ becomes position-independent as in Eq. (17), thus the phase of the reflected neutron factors out of the volume integral in Eq. (23). Hence, $P^{\mu\mu'\nu\nu'}$ is given by

$$\lim_{t\to\infty}P^{\mu\mu'\nu\nu'}(t) = \Lambda_{\mu\mu'\nu\nu'}\, e^{i\eta_{\mu\mu'\nu\nu'}}, \tag{24}$$

where $\Lambda_{\mu\mu'\nu\nu'}$ encodes the overlappings between reflected spin states at the detector, given by

$$\Lambda_{\mu\mu'\nu\nu'} = A_{\nu\nu'}\, e^{-\frac{((\mu'-\mu)\xi_z^{(\mathrm{i})}+2\tilde{\lambda}_{z\nu}-2\tilde{\lambda}_{z\nu'})^2}{2(\Delta_{z\nu}^2+\Delta_{z\nu'}^2)}-\frac{(\mu-\mu')^2\xi_x^{(\mathrm{i})2}}{4\Delta_x^2}} \tag{25}$$

$A_{\nu\nu'} = \sqrt{\frac{2\pi\mathcal{N}^*_{z\nu}\mathcal{N}_{z\nu'}}{\mathcal{N}_{z\nu}\mathcal{N}^*_{z\nu'}(\Delta^2_{z\nu}+\Delta^2_{z\nu'})}}$, $\Delta_{z\nu}$ is defined in Eq. (16) with the ν index denoting the corresponding spin-dependent $\widetilde{W}$ and the asymptotic reflected phase difference, $\eta_{\mu\mu'\nu\nu'}\in\mathbb{R}$

$$\eta_{\mu\mu'\nu\nu'} = S_{\mu\nu} - S_{\mu'\nu'} \tag{26}$$

where $S_{\mu\nu} = S_\nu - \frac{\mu}{2}\widetilde{\mathbf{k}}_0\cdot\boldsymbol{\xi}^{(\mathrm{i})}$ with S_ν given in Eq. (17).

For experimental attempts to observe the GH-shift for neutron, such as [6], it will be simplest to align the original entangled spin states with the eigen spin state of the surface. This set up simplifies the polarization in Eq. (22) due to $\mathbf{U}_{\mu\nu} = \delta_{\mu\nu}$. For example,

$$P_x = \Lambda_{+-+-}\cos(S_{++} - S_{--}) \tag{27}$$

assuming that the entangled quantization axis $\hat{n} = \hat{z}$. We see that the GH-shift can be extracted from both terms in Eq. (27). Specifically, Λ_{+-+-} contains the difference in the spin states's penetration depths $\lambda_{z+} - \lambda_{z-}$ at the surface because their wave packets no longer have perfect overlapping at the detector leading to this source of depolarization. One can then extract $\lambda_{x+} - \lambda_{x-}$ since the two differences are related by a modified trigonometric relationship in Eq. (15). Meanwhile, the reflection phase difference $S_{++} - S_{--}$ can be used with the modified ACH formula Eq. (18) to also obtain $\lambda_{x+} - \lambda_{x-}$. [Quan: Interestingly, if one is agnostic about the wave packet nature of the incoming beam and thus identify the plane wave reflection phase shift $\Phi = S$ extracted from P_x combined with the magnetic layers structure, and if the $\widetilde{W}$-correction is observed, then this will certify that the incoming state is a wave packet.]

Entangled-Beam Reflectrometry.—

Probing surface physics with entangled beams.—

We now consider the case where the spatial variation of $\hat{V}$ is no longer constrained to be along $\hat{z}$, i.e. $\hat{V}(\mathbf{r})$ where hereinafter $\mathbf{r} = (x,y,z) = (\mathbf{r}_\parallel, z)$ and similarly for other vector quantities. Generally, one has to solve the full Schrödinger equation to obtain the reflection operator, but here we consider the limit when the transverse variation of $\hat{R}$ on the surface is much smaller than the incoming wave packet widths $\Delta_{l/t}$. For an unentangled neutron, this entails that the entire neutron wave packet only samples the local constant $\hat{R}$, reducing the problem to the case discussed above. Nevertheless, for an entangled beam due to the presence of $\boldsymbol{\xi}^{(\mathrm{i})}$, another length scale emerges. Particularly, if $\xi_\parallel^{(\mathrm{r})}$ is significantly larger than $\hat{R}(\mathbf{r}_\parallel)$'s spatial variation, the two spin states effectively sample $\hat{R}(\mathbf{r}_{s\parallel\uparrow})$ and $\hat{R}(\mathbf{r}_{s\parallel\downarrow})$ on the surface, where the two impact locations are respectively $\mathbf{r}_{s\parallel\uparrow}$ and $\mathbf{r}_{s\parallel\uparrow}$, separated by $\boldsymbol{\xi}_\parallel^{(\mathrm{r})}$. Hence, we see that other physical quantities derived from $\hat{R}(\mathbf{r}_\parallel)$, such as $\widetilde{\Phi}$, $\tilde{\lambda}$, $\widetilde{W}$ and $\mathbf{U}$, also depend on $\mathbf{r}_\parallel$. The measured polarization can be obtained straightforwardly by using Eq. (22) with these now $\mathbf{r}_\parallel$-dependent quantities, the details of deriving $\vec{P}$ are given in Appendix. B.

Assessing the mathematical structure of Eq. (22), we see that $\vec{P}$ of an incoming entangled beam in Eq. (19)

contains information about the effective magnetic correlation of the surface on the length scale of $\xi_{\parallel}^{(i)}$. Particularly, $\mathbf{U}(\mathbf{r}_{\parallel})$ encodes the effective magnetic field direction at $\mathbf{r}_{\parallel}$, while $\eta(\mathbf{r}_{\parallel})$ is the associating reflection phase difference. [Quan: We demonstrate in Fig. **??** that for surfaces with 1D and 2D periodic magnetic structures, there is a strong dependence of the surface period in our spin-echo signal. The dependence increases dramatically as the grating incidence is getting close to the critical angle, because the reflecting phase varies drastically.]

Conclusions.— ff

[1] I. Newton, *Philosophiae Naturalis Principia Mathematica* (Harvard University Press, Cambridge, 1972).
[2] F. Goos and H. Hänchen, *Ein neuer und fundamentaler versuch zur totalreflexion*, Ann. Phys. **436**, 333 (1947).
[3] F. Goos and H. Hänchen, *Neumessung des strahlversetzungseffektes bei totalreflexion*, Ann. Phys. **440**, 251 (1949).
[4] K. Artmann, *Berechnung der seitenversetzung des totalreflektierten strahles*, Ann. Phys. **437**, 87 (1948).
[5] J. L. Carter and H. Hora, *Total reflection of matter waves: The Goos–Hänchen effect for grazing incidence*, J. Opt. Soc. Am. **61**, 1640 (1971).
[6] V.-O. de Haan *et. al.*, *Observation of the Goos-Hänchen shift with neutrons*, Phys. Rev. Lett. **104**, 010401 (2010).
[7] Rémi H. Renard, *Total reflection: A new evaluation of the Goos–Hänchen shift*, J. Opt. Soc. Am. **54**, 1190 (1964).
[8] Helmut K. V. Lotsch, *Reflection and refraction of a beam of light at a plane interface*, J. Opt. Soc. Am. **58**, 551-561 (1968).
[9] C.-F. Li, *Unified theory for Goos-Hänchen and Imbert-Fedorov effects*, Phys. Rev. A **76**, 013811 (2007).
[10] B. Bhaduri, M. Yessenov and A. F. Abouraddy, *Anomalous refraction of optical spacetime wave packets*, Nat. Photonics **14**, 416–421 (2020).
[11] N.K. Pleshanov, *Spin particles at stratified media: operator approach*, Z. Phys. B **100**, 423—427 (1996).
[12] V.K. Ignatovich, *Neutron reflection from condensed matter, the Goos–Hänchen effect and coherence*, Phys. Lett. A **322**, 36 (2004).
[13] A. I. Frank, *On the Goos-Hänchen effect in neutron optics*, J. of Phys.: Conference Series **528**, 012029 (2014).
[14] J. L. Agudín, *Time delay of scattering processes*, Phys. Rev. **171**, 1385 (1968).
[15] A. A. Md Irfan, P. Blackstone, R. Pynn, and G. Ortiz, *Quantum Entangled-Probe Scattering Theory*, New J. Phys. **23**, 083022 (2021).
[16] K. Yasumoto and Y. Ōishi, *A new evaluation of the Goos–Hänchen shift and associated time delay*, J. App. Phys. **54**, 2170 (1983).
[17] D. A. Pushin, M. Arif, M. G. Huber, and D. G. Cory, PRL **100**, 250404 (2008)
[18] Supplemental Material.

SUPPLEMENTAL MATERIAL: ENTANGLED-BEAM REFLECTOMETRY AND GOOS-HÄNCHEN SHIFT

G. Ortiz*, Q. Le Thien and R. Pynn

In what follows, we expand on various aspects.

Appendix A: Neutron optics with spin

In the following we are assuming the optical potential approximation, where the medium represents a constant (spin or polarization dependent) refractive index. We follow the operator approach developed in Ref. [11]. The magnetic structures along the z-axis are simply characterized by a stratified medium with layers, labeled by the index $j = 0, 1, \cdots, N+1$, and potential energy given by

$$\hat{V}_j = V_j - \mu_{\mathsf{n}}\, \boldsymbol{\sigma} \cdot \mathbf{B}_j. \tag{A1}$$

Here, V_j is a scalar potential, $\mu_{\mathsf{n}} < 0$ for neutrons, $\boldsymbol{\sigma} = (\sigma_x, \sigma_y, \sigma_z)$ are Pauli matrices and $\hat{\mathbf{b}}_j = \mathbf{B}_j/|\mathbf{B}_j|$ is the magnetic field unit vector (see Fig. 1).

The spinor state and its first derivative in layer j are given by

$$\begin{aligned}\Psi_j(z) &= e^{i\mathsf{k}_j z}\chi_j^+ + e^{-i\mathsf{k}_j z}\chi_j^- \\ \Psi_j'(z) &= i\mathsf{k}_j(e^{i\mathsf{k}_j z}\chi_j^+ - e^{-i\mathsf{k}_j z}\chi_j^-),\end{aligned} \tag{A2}$$

which can be compactly written as

$$\begin{pmatrix}\Psi_j(z)\\ \Psi_j'(z)\end{pmatrix} = \mathsf{B}_j(z)\,\boldsymbol{\chi}_j = \begin{pmatrix} e^{i\mathsf{k}_j z} & e^{-i\mathsf{k}_j z} \\ i\mathsf{k}_j e^{i\mathsf{k}_j z} & -i\mathsf{k}_j e^{-i\mathsf{k}_j z}\end{pmatrix}\boldsymbol{\chi}_j\ , \tag{A3}$$

where the momentum operator,

$$\mathsf{k}_j = \frac{k_j^+ + k_j^-}{2} + \frac{k_j^+ - k_j^-}{2}\,\boldsymbol{\sigma}\cdot\hat{\mathbf{b}}_j, \tag{A4}$$

has eigenvalues $k_j^{\pm} = \sqrt{2m(E_\perp - (V_j \mp \mu_{\mathsf{n}}|\mathbf{B}_j|))}$ ($\hbar = 1$), and the (two-component) spinor

$$\boldsymbol{\chi}_j = \begin{pmatrix}\chi_j^+\\ \chi_j^-\end{pmatrix} \tag{A5}$$

is expressed in terms of unnormalized spin-1/2 states $\chi_j^{\pm}$.

Using the transfer matrix

$$\begin{pmatrix}\Psi_j(z_{j-1})\\ \Psi'_j(z_{j-1})\end{pmatrix} = \mathsf{M}_j \begin{pmatrix}\Psi_j(z_j)\\ \Psi'_j(z_j)\end{pmatrix}, \tag{A6}$$

one can connect the spinor state at coordinates z_j and z_{j-1}. From boundary conditions at z_{j-1} and z_j in layer j

$$\begin{pmatrix}\Psi_j(z_{j-1})\\ \Psi'_j(z_{j-1})\end{pmatrix} = \mathsf{B}_{j-1}(z_{j-1})\boldsymbol{\chi}_{j-1} = \mathsf{B}_j(z_{j-1})\boldsymbol{\chi}_j \tag{A7}$$

$$\begin{pmatrix}\Psi_j(z_j)\\ \Psi'_j(z_j)\end{pmatrix} = \mathsf{B}_j(z_j)\boldsymbol{\chi}_j = \mathsf{B}_{j+1}(z_j)\boldsymbol{\chi}_{j+1}, \tag{A8}$$

it results

$$\begin{aligned}\begin{pmatrix}\Psi_j(z_{j-1})\\ \Psi'_j(z_{j-1})\end{pmatrix} &= \mathsf{B}_j(z_{j-1})\mathsf{B}_j^{-1}(z_j)\begin{pmatrix}\Psi_j(z_j)\\ \Psi'_j(z_j)\end{pmatrix}\\ &= \mathsf{M}_j\begin{pmatrix}\Psi_j(z_j)\\ \Psi'_j(z_j)\end{pmatrix},\end{aligned} \tag{A9}$$

with $(d_j = z_j - z_{j-1})$

$$\mathsf{B}_j^{-1}(z) = \frac{1}{2}\begin{pmatrix} e^{-i\mathsf{k}_j z} & -ie^{-i\mathsf{k}_j z}\mathsf{k}_j^{-1}\\ e^{i\mathsf{k}_j z} & ie^{i\mathsf{k}_j z}\mathsf{k}_j^{-1}\end{pmatrix}, \tag{A10}$$

and

$$\mathsf{M}_j = \begin{pmatrix}\cos(\mathsf{k}_j d_j) & -\sin(\mathsf{k}_j d_j)\mathsf{k}_j^{-1}\\ \mathsf{k}_j\sin(\mathsf{k}_j d_j) & \cos(\mathsf{k}_j d_j)\end{pmatrix}, \tag{A11}$$

where the inverse of the momentum operator is

$$\mathsf{k}_j^{-1} = \frac{1}{k_j^+ k_j^-}\left(\frac{k_j^+ + k_j^-}{2} - \frac{k_j^+ - k_j^-}{2}\,\boldsymbol{\sigma}\cdot\hat{\mathbf{b}}_j\right), \tag{A12}$$

In the case where there are N magnetic layers

$$\begin{pmatrix}\Psi(z_0)\\ \Psi'(z_0)\end{pmatrix} = \mathsf{M}\begin{pmatrix}\Psi(z_N)\\ \Psi'(z_N)\end{pmatrix}, \tag{A13}$$

where $\mathsf{M} = \mathsf{M}_1\mathsf{M}_2\cdots\mathsf{M}_N$ and, in general, $[\mathsf{M}_j, \mathsf{M}_{j'}] \neq 0$. They commute whenever $\mathbf{B}_j$ in different layers are collinear, i.e., $[\boldsymbol{\sigma}\cdot\hat{\mathbf{b}}_j, \boldsymbol{\sigma}\cdot\hat{\mathbf{b}}_{j'}] = 2i(\hat{\mathbf{b}}_j \wedge \hat{\mathbf{b}}_{j'})\cdot\boldsymbol{\sigma} = 0$.

One can define reflection $\hat{R}$ and transmission $\hat{T}$ operators

$$\begin{aligned}\Psi_R(z_0) &= \hat{R}\,\Psi_0(z_0) = e^{-ik_{0z}z_0}\chi_0^-,\\ \Psi_T(z_N) &= \hat{T}\,\Psi_0(z_0) = e^{i\mathsf{k}_N z_N}\chi_N^+,\end{aligned} \tag{A14}$$

by its action on $\Psi_0(z_0) = e^{ik_{0z}z_0}\chi_0^+$ with $\Psi(z_0) = \Psi_0(z_0) + \Psi_R(z_0)$ and $\Psi(z_N) = \Psi_T(z_N)$. These operators can be expressed in terms of the operator M as

$$\begin{aligned}\hat{T} &= (\mathsf{M}_{11} + i\mathsf{M}_{12}\mathsf{k}_N)^{-1}(\mathbb{1} + \hat{R}),\\ \hat{R} &= (k_{0z} + \boldsymbol{\kappa})^{-1}(k_{0z} - \boldsymbol{\kappa}),\end{aligned} \tag{A15}$$

where $\boldsymbol{\kappa} = -i(\mathsf{M}_{21} + i\mathsf{M}_{22}\mathsf{k}_{N+1})(\mathsf{M}_{11} + i\mathsf{M}_{12}\mathsf{k}_{N+1})^{-1}$.

In the TIR situation the operator $\hat{R}$ has to be unitary. That means that the basis that diagonalizes $\hat{R}$ must also diagonalize the operator $\boldsymbol{\kappa}$

$$\hat{R} = \mathbf{U}\,\mathrm{diag}(R_+, R_-)\,\mathbf{U}^{-1}, \tag{A16}$$

where

$$R_\pm = \frac{k_{0z} - \kappa_\pm}{k_{0z} + \kappa_\pm} = e^{-2i\phi_\pm}, \tag{A17}$$

and $\kappa_\pm \in \mathbb{C}$ are the eigenvalues of $\boldsymbol{\kappa}$. Since the eigenvalues of a unitary operator have modulus 1, this implies that $\kappa_\pm$ are purely imaginary.

1. Wave Packet

For a more realistic scenario where the longitudinal coherence length of the neutron is small relative to the GH shift, we need a wave packet treatment. For the sake of simplicity, we choose Δ to be the width of the wave packet when the neutron arrives at the interface, meaning $z_0 = 0$. Similar to the constant beam case, in order to find the reflected wave function, we have to carry out the Fourier transformation to momentum space

$$\Psi^{(i)}_{z<0}(\vec{r},0) = \mathcal{N}\int d^3q\ \exp\left[i\left(\mathbf{k}\cdot\vec{r} - E_q t\right)\right]\exp\left[-\frac{\Delta^2}{2}\left(k_z - k_{0z}\right)^2 - \frac{\Delta}{2}\right.$$

(A18)

Using reflection coefficient for each $\mathbf{k}$ state in Eq. (**??**), we obtain the reflection wave function

$$\Psi^{(r)}_{z<0}(\vec{r},t) = \mathcal{N}\int d^3q\ \exp\left[i\left(\mathbf{k}\cdot\vec{r} - E_q t\right)\right]\exp\left[-\frac{\Delta^2}{2}\left(k_z - k_{0z}\right)^2 - \frac{\Delta}{2}\right.$$

(A19)

Similar to the constant beam case, this integral also does not in a closed form. Hence, one needs to use the approximation scheme in Eq. (**??**). However, the crucial difference is that since in the wave packet treatment, the momenta k_z is an independent variable and the reflection coefficient $r^\pm(\mathbf{k})$ is a function of all 3 components of $\mathbf{k}$, we need to expand $\ln r^\pm(\mathbf{k})$ at $\mathbf{k} = \mathbf{k}$.

$$\ln\left[r^\pm(\mathbf{k})\right] \simeq \ln\left[r^\pm(k_{0z})\right] + \frac{2\left(k_{0z} - k_z\right)}{\sqrt{k_{0z}^2 - 2mV}} \tag{A20}$$

Interestingly, since k_z is now a separate variable, there is no further dependence on $q_\parallel$ in $r^\pm$. Therefore, the expansion now is performed with respect k_z, implying that the expansion order is with respect to the longitudinal coherence length rather than the transverse as in the constant beam case. We obtain the shift in z-direction

$$\xi_z^\pm = \frac{1}{i}\frac{d}{dk_z}\left[\ln r^\pm(k_z))\right]\Big|_{k_z=k_{0z}} = \frac{2i}{\sqrt{k_{0z}^2 - 2mV}} = \frac{2i}{k_{0z}^\pm} = 2\lambda \tag{A21}$$

where λ is the penetration depth of the boundary. To obtain the GH shift we need to solve the kinematic equations for when the wave packet center crosses the boundary $z = O$

$$t^\pm = \frac{\xi_z^\pm}{v_z} = \frac{\xi_z^\pm}{k_{0z}/m} \tag{A22}$$

Surprisingly, this yields the same result as the constant beam approximation. However, one fundamental difference is the expansion order of the exponent.

$$\lambda_x^{\pm} = v_x t = \frac{k_{0x}}{m} t = \frac{k_{0x}\xi_z}{k_{0z}} = \frac{2ik_{0x}}{k_{0z}k_z^{\pm}} \tag{A23}$$

2. 2nd-order correction to the GH-shift

We see that in the limit $t \to \infty$, the incoming wavefunction $\Psi^{(\mathsf{r})}_{z<0}(\vec{r},t)$ disappears and the reflected wavefunction $\Psi^{(\mathsf{r})}_{z<0}(\vec{r},t)$ dominates. Assuming that the momentum distribution does not have substantial distribution over the classical transmission regime, aka the penetration depth λ is real, leading to $|r(k_z)| = 1$ we can write the reflected momentum wavefunction up to second-order around the peak momentum k_{0z} as

$$\Psi^{(\mathsf{r})}(k_z,t) = \mathcal{N} r(k_{0z})\, e^{-2ik_{0z}\lambda_z} \exp\left[-ik_z(z+z_0-2\lambda_z) - \frac{\Delta^2}{2}(k_z-k_{0z})^2 - i\frac{k_z^2}{2m}t + i\lambda^3 k_{0z}(k_z-k_{0z})^2\right] \tag{A24}$$

After carrying out the gaussian integral to invert back to real space, we obtain the wavefunction

$$\Psi^{(\mathsf{r})}(z,t) = \mathcal{N}(t) r(k_{0z})\, e^{-2ik_{0z}\lambda_z} \exp\left[\phi^{(2)}(z,t)\right] \tag{A25}$$

where the normalization factor in real space is given by

$$\mathcal{N}(t) = \Delta\left[1 + \frac{i}{m\Delta^2}\left(t - 2mk_{0z}\lambda_z^3\right)\right]^{-\frac{1}{2}} \tag{A26}$$

We can extract the GH-shift via analyzing $\mathrm{Re}(\phi(z,t))$ to obtain

$$\mathrm{Re}\left[\phi^{(2)}(z,t)\right] = \frac{-\left(z+z_0-2\lambda_z+\frac{k_{0z}}{m}t\right)^2}{2\Delta^2\left[1+\frac{1}{m^2\Delta^4}\left(t-2mk_{0z}\lambda_z^3\right)^2\right]} \tag{A27}$$

where we see that the second-order correction does not affect the GH-shift. However, if we examine the diffusion of the reflected wavepacket width, we see that the deffusing time is delayed by $2mk_{0z}\lambda_z^3$ relative to the free-propagating incoming wave, effectively reducing the reflected wavepacket width.

We now turn to analyze the phase accumulated by the reflected wave via examining $\mathrm{Im}\left[\phi^{(2)}(z,t)\right]$ in the limit $t \to \infty$

$$\lim_{t\to\infty} \mathrm{Im}\left[\phi^{(2)}(z,t)\right] = \frac{k_{0z}^2}{2m}t - k_{0z}(z_0+\delta z) + 2k_{0z}\lambda_z + 4k_{0z}^3\lambda_z^3 \tag{A28}$$

where we keep only non-vanishing terms as $t \to \infty$ via the substitution $z \to k_{0z}t/m + \delta z$ and the first term is the usual kinetic phase associated with the free propagation. The overall accumulated phase can be easily obtained now by realizing that

$$\lim_{t\to\infty} \mathcal{N}(t) = |\mathcal{N}(t)| e^{-i\frac{\pi}{4}} \tag{A29}$$

meaning that it is simply an overall unobservable phase in the asymptotic limit. The total phase is straightforwardly given by

$$\lim_{t\to\infty} \mathrm{Arg}\left[\Psi^{(\mathsf{r})}(t)\right] = \frac{1}{i}\ln\left[r(k_{0z})\right] + 4k_{0z}^3\lambda_z^3 \tag{A30}$$

We see that from the wavepacket approach, the lateral GH-shift comes from the semi-classical interpretation that the wavepacket goes into and backs out of the material the penetration depth λ_z. This can be traced back to the first-order term in Eq. (A24), resulting in the second term here. Interestingly, de Haan et al.'s claim of observation of the GH-shift relies only upon the first-term in this expansion [1]. Furthermore, we have shown here how to recover the usual planewave analysis of the GH-shift via a proper consideration of the wavepacket dynamics in the asymptotic approach.

We are interested in the phase shift in Eq. (17), because the Artmann-Carter-Hora formula for the lateral GH-shift is derived from this phase. More importantly, if one relies on the phase shift of the neutron to extrapolate the lateral GH-shift, the correction terms up to $\mathcal{O}\left(k_{0z}^4\lambda^4\right)$ as derived will yield additional terms to this perceived lateral GH-shift

$$\lambda_x^{\mathrm{ACH}} = \frac{k_{0x}}{k_{0z}}\frac{d\phi}{dk_{0z}} \approx \frac{k_{0x}}{k_{0z}}\left(2\lambda_z + 12k_c^2k_{0z}^2\lambda_z^5\right) \tag{A31}$$

where the first term is the usual result for the lateral GH-shift, which is usually claimed to show the equivalence between the ACH formula and other derivations of the lateral GH-shift. However, if we take the GH-shift as a geometrical quantity, defined by tracking the neutron's asymptotic trajectory, we see that such corrections are not there as shown previously in Eq. (A27). We have shown here that even if one includes higher-order corrections due to the spread of the wavefunction, the geometrical GH-shift remains the same. In other words, if one is to measure the lateral GH-shift via the phase accumulated by the neutron, one has to modify the ACH formula

$$\lambda_x = \frac{k_{0x}}{k_{0z}}\left(\frac{d\phi}{dk_{0z}} - 12k_c^2k_{0z}^2\lambda_z^5\right) \tag{A32}$$

While the previous treatment applies for a scalar field, it is straightforward to extend that to the spinor case for neutrons, where the previous scalar field becomes the spinor components along the direction of the magnetic field. If one relies on measuring the relative phase between the two spinor components to infer the GH-shift, we see that the polarization of the neutron in the asymp-

totic limit is in the form

$$P_x = \int d\delta z \langle \vec{\sigma} \rangle = \cos\left[\mathrm{Arg}\left(\Psi_\uparrow^{(\mathrm{r})}(t)\right) - \mathrm{Arg}\left(\Psi_\downarrow^{(\mathrm{r})}(t)\right)\right] \int d\delta z \; |\mathcal{N}|^2 \exp\left[-\frac{(\delta z + z_0 - 2\lambda_{z\uparrow})^2}{t^2/m^2\Delta^2} - \frac{(\delta z + z_0 - 2\lambda_{z\downarrow})^2}{t^2/m^2\Delta^2}\right]$$
$$= \exp\left[-\frac{2\left(\lambda_{z\downarrow} - \lambda_{z\uparrow}\right)^2}{t^2/m^2\Delta^2}\right] \cos\left[\mathrm{Arg}\left(\Psi_\uparrow^{(\mathrm{r})}(t)\right) - \mathrm{Arg}\left(\Psi_\downarrow^{(\mathrm{r})}(t)\right)\right] \tag{A33}$$

where we used the fact that in the far-field asymptotic limit, the phase of the outgoing wavefunction has a trivial planewave-dependence on δz.

Appendix B: Probing Surface Magnetic Field

After promoting the reflection operator $\hat{R}(\mathbf{r}_\parallel)$, the reflected wave function for an entangled incoming state in Eq. (19) is given by

$$\Psi_{\boldsymbol{\xi}}^{(\mathrm{r})}(\mathbf{r}, t) = \int d\mathbf{k}\; \Psi^{(\mathrm{i})}(\mathbf{k}) e^{i(\mathbf{k}^{(\mathrm{r})}\cdot\mathbf{r} - \frac{k^{(\mathrm{r})2}}{2m}t)}(\mathbf{k}) \tag{B1}$$
$$\sum_{\mu\nu'} \hat{R}_\nu\left(\mathbf{r}_{s\parallel} + \mu\frac{\boldsymbol{\xi}_\parallel}{2}, k_z\right) \delta_{\nu\nu'} \mathbf{U}^\dagger_{\nu'\mu}\left(\mathbf{r}_{s\parallel} + \mu\frac{\boldsymbol{\xi}_\parallel}{2}\right) e^{-i\mu\mathbf{k}\cdot\boldsymbol{\xi}^{(i)}/2} |\mu\rangle$$
$$= \sum_{\mu,\nu=\pm} \mathbf{U}^*_{\mu\nu}\left(\mathbf{r}_{s\parallel} + \mu\frac{\boldsymbol{\xi}_\parallel}{2}\right) \Psi^{(\mathrm{r})}_{\mu\nu}(\mathbf{r}_{s\parallel}, \mathbf{r}, t) \otimes |\nu\rangle$$

where the $\mathbf{r}_{s\parallel}$-dependence indicates the midpoint between the spin states impact parameter on the surface. Here, we write these impact parameters explicitly, but they indeed depends on the initial wavepacket center position $\mathbf{r}_c$ and the mean momentum $\mathbf{k}_0$.

The polarization is then given by

$$\vec{P}_{\boldsymbol{\xi}}(\mathbf{r}_{s\parallel}) = \tfrac{1}{2} \sum_{\mu,\mu',\nu,\nu'=\pm} \mathbf{U}_{\mu\nu}\left(\mathbf{r}_{s\parallel} + \mu\frac{\boldsymbol{\xi}_\parallel}{2}\right) \mathbf{U}^*_{\mu'\nu'}\left(\mathbf{r}_{s\parallel} + \mu'\frac{\boldsymbol{\xi}_\parallel}{2}\right)$$
$$\langle\nu(\mu)|\,\vec{\sigma}\,|\nu'(\mu')\rangle\, P^{\mu\mu'\nu\nu'} \tag{B3}$$

where $P^{\mu\mu'\nu\nu'} \equiv \lim_{t\to\infty} P^{\mu\mu'\nu\nu'}(t)$ and the notation $|\nu(\mu)\rangle$ indicates that the spin basis $|\nu\rangle$ at the reflection point depends on the position on the surface $\mathbf{r}_{s\parallel} \pm \mu\boldsymbol{\xi}_{s\parallel}$. The matrix element $\langle\nu|\,\vec{\sigma}\,|\nu'\rangle$ is explicitly given by

$$\langle\nu(\mu)|\,\vec{\sigma}\,|\nu'(\mu')\rangle$$
$$= \sum_{\mu,\mu'} \langle\mu|\,\mathbf{U}^{T*}_{\nu\mu}\left(\mathbf{r}_{s\parallel} + \mu\frac{\boldsymbol{\xi}_\parallel}{2}\right) \vec{\sigma} \mathbf{U}^T_{\nu'\mu'}\left(\mathbf{r}_{s\parallel} + \mu'\frac{\boldsymbol{\xi}_\parallel}{2}\right) |\mu'\rangle$$
$$= \sum_{\mu\mu'} \mathbf{U}^{T*}_{\nu\mu}\left(\mathbf{r}_{s\parallel} + \mu\frac{\boldsymbol{\xi}_\parallel}{2}\right) \vec{\sigma}_{\mu\mu'} \mathbf{U}_{\mu'\nu'}\left(\mathbf{r}_{s\parallel} + \mu'\frac{\boldsymbol{\xi}_\parallel}{2}\right)$$
$$= \left[\mathbf{U}^\dagger\left(\mathbf{r}_{s\parallel} + \mu\frac{\boldsymbol{\xi}_\parallel}{2}\right) \vec{\sigma} \mathbf{U}\left(\mathbf{r}_{s\parallel} + \mu'\frac{\boldsymbol{\xi}_\parallel}{2}\right)\right]_{\nu\nu'} \tag{B4}$$

There is a normalization issue of the outgoing wave function that we need to be careful about. We will show here that even though we started out with a normalized wave function as Eq. (19), $\Psi^{(\mathrm{r})}_{\boldsymbol{\xi}}(\mathbf{r}, t)$ is unnormalized. The normalization factor is given by

$$\frac{1}{|\mathcal{N}(\boldsymbol{\xi}, \mathbf{r}_{s\parallel})|^2} = \int d^2\mathbf{r}\, |\Psi^{(\mathrm{r})}_{\boldsymbol{\xi}}(\mathbf{r}, t)|^2$$
$$= \frac{1}{2} \sum_{\mu,\mu',\nu,\nu'=\pm} \mathbf{U}_{\mu\nu}\left(\mathbf{r}_{s\parallel} + \mu\frac{\boldsymbol{\xi}_\parallel}{2}\right) \mathbf{U}^*_{\mu'\nu'}\left(\mathbf{r}_{s\parallel} + \mu'\frac{\boldsymbol{\xi}_\parallel}{2}\right)$$
$$\langle\nu(\mu)|\,\vec{\sigma}\,|\nu'(\mu')\rangle\, P^{\mu\mu'\nu\nu'}$$
$$= \frac{1}{2} \sum_{\mu,\mu',\nu,\nu'=\pm} \mathbf{U}_{\mu\nu}\left(\mathbf{r}_{s\parallel} + \mu\frac{\boldsymbol{\xi}_\parallel}{2}\right) \mathbf{U}^*_{\mu'\nu'}\left(\mathbf{r}_{s\parallel} + \mu'\frac{\boldsymbol{\xi}_\parallel}{2}\right)$$
$$\left[\mathbf{U}^\dagger\left(\mathbf{r}_{s\parallel} + \mu\frac{\boldsymbol{\xi}_\parallel}{2}\right) \mathbf{U}\left(\mathbf{r}_{s\parallel} + \mu'\frac{\boldsymbol{\xi}_\parallel}{2}\right)\right]_{\nu\nu'} P^{\mu\mu'\nu\nu'} \tag{B5}$$

As an example, we consider the specific case of a neutron spatially separated by $\boldsymbol{\xi}_{s\parallel} = \xi_0\hat{x}$ and the two spin states' impact location has magnetic fields $\vec{B}(\mathbf{r}_{s\parallel} + \boldsymbol{\xi}_\parallel/2) = B_0\hat{x}$ and $\vec{B}(\mathbf{r}_{s\parallel} - \boldsymbol{\xi}_\parallel/2) = B_0\hat{y}$, implying $\mathbf{U}(\mathbf{r}_{s\parallel} + \boldsymbol{\xi}_\parallel/2) = \hat{U}_x$ and $\mathbf{U}(\mathbf{r}_{s\parallel} - \boldsymbol{\xi}_\parallel/2) = \hat{U}_y$. Because the magnetic field has the same magnitude, the reflection operators have the same form $\hat{R} = \mathrm{diag}(e^{i\phi_+}, e^{i\phi_-})$ with respect to their own bases, but they are different operators. The normalization for such scenario is given by

$$|\mathcal{N}(\boldsymbol{\xi}, \mathbf{r}_{s\parallel})|^2 = \frac{1}{2}\left[2 + \cos k_x\xi + \sqrt{2}\sin k_x\xi \sin\left(\phi_+ - \phi_- + \frac{\pi}{4}\right)\right] \tag{B6}$$

which in general can be greater or less than 1 depending on the entangled length ξ. This breakdown of unitarity is due to the fact that in prescribing the interaction to sample to local magnetic field at each spin state's impact location on the surface, we are breaking the $SU(2)$ symmetry between the entangled bases $|\uparrow\rangle$ and $|\downarrow\rangle$, thus the unitarity associated with the $SU(2)$ is lost. One can also see via the operator form of the operator that we are carrying out here

$$\mathcal{O} = \sum_\mu U\left(\mathbf{r} + \mu\frac{\boldsymbol{\xi}}{2}\right) |\mu\rangle\langle\mu| \tag{B7}$$

where U is the local unitary operator at each impact point. Hence, this interferometric model clearly involves non-unitary operations.

Therefore, we have to re-normalize the reflecting wavefunction such that the polarization is given by

$$\vec{P}_{\boldsymbol{\xi}}^{\,\mathrm{obs}}(\mathbf{r}_{s\parallel}) = \frac{\vec{P}_{\boldsymbol{\xi}}(\mathbf{r}_{s\parallel})}{|\mathcal{N}(\boldsymbol{\xi}, \mathbf{r}_{s\parallel})|^2} \tag{B8}$$

Nonetheless, because for neutrons we do not have control over individual neutron's impact parameters, this means that the observed signal needs to be further averaged over the impact parameter distribution, assumed to be uniform here across the beam. Here, if we consider an infinite periodic structure with a period κ on the surface,

the observed polarization is then given by

$$\vec{P}_{\boldsymbol{\xi}}^{\,\mathrm{obs}} = \frac{1}{\kappa}\int d\mathbf{r}_{s\parallel}\vec{P}_{\boldsymbol{\xi}}^{\,\mathrm{obs}}(\mathbf{r}_{s\parallel}) \tag{B9}$$

$$\vec{P}_{\boldsymbol{\xi}}^{\,\mathrm{obs}} = \frac{1}{\kappa^2}\int d^2\mathbf{r}_{s\parallel}\vec{P}_{\boldsymbol{\xi}}^{\,\mathrm{obs}}(\mathbf{r}_{s\parallel}) \tag{B10}$$

for 1D and 2D periodic structure respectively, where the integrals are over one period κ.